optimum velocity would be desirable for visually mediated flight stabilization during hovering, when images are nearly stationary. However, optical constraints to the spatial acuity of insect compound eyes mean that a lower velocity optimum would not be attainable without impractically large correlation delays. Nevertheless, it seems that in insects, as in humans, the neural mechanisms for motion detection are matched, as far as possible, to motion experienced during behaviour. □

Received 27 February; accepted 21 May 1996.

1. Egelhaaf, M., Borst, A. & Reichardt, W. *J. opt. Soc. Am.* A **6,** 1070–1087 (1989).
2. Borst, A. & Egelhaaf, M. *Trends Neurosci.* **12,** 297–306 (1989).
3. Buchner, E. in *Photoreception and Vision in Invertebrates* (ed. Ali, M. A.) 561–621 (Plenum, New York, 1984).
4. Hassenstein, B. & Reichardt, W. *Z. Naturf.* B **11,** 513–524 (1956).
5. Reichardt, W. *Z. Naturf.* B **12,** 448–457 (1957).
6. Reichardt, W. in *Principles of Sensory Communication* (ed. Rosenblith, W. A.) 303–317 (Wiley, New York, 1961).
7. Barlow, H. B. & Levick, W. R. *J. Physiol., Lond.* **178,** 477–504 (1965).
8. Wolf-Oberhollenzer, F. & Kirschfeld, K. *J. Neurophysiol.* **71,** 1559–1573 (1994).
9. Wilson, H. R. *Biol. Cybern.* **51,** 213–222 (1985).
10. Santen, J. P. H. van & Sperling, G. *J. opt. Soc. Am.* A **2,** 300–321 (1985).
11. Maddess, T. & Laughlin, S. B. *Proc. R. Soc. Lond.* B **225,** 251–275 (1985).
12. Ruyter van Steveninck, R. de, Zaagman, W. H. & Mastebroek, H. A. K. *Biol. Cybern.* **54,** 223–236 (1986).
13. Maddess, T., DuBois, R. A. & Ibbotson, M. R. *J. exp. Biol.* **161,** 171–199 (1991).
14. Hausen, K. & Egelhaaf, M. in *Facets of Vision* (eds Stavenga, D. & Hardie, R. C.) 391–444 (Springer, Berlin, 1989).
15. Farina, W. M., Varju, D. & Zhou, Y. *J. comp. Physiol.* A **174,** 239–247 (1994).
16. Ibbotson, M. R. & Goodman, L. J. *J. exp. Biol.* **148,** 255–279 (1990).
17. Bidwell, N. J. & Goodman, L. J. *Apidologie* **24,** 333–354 (1993).
18. Kelly, D. H. *J. opt. Soc. Am.* A **69,** 1340–1349 (1979).
19. Burr, D. C. & Ross, J. *Vision Res.* **22,** 479–484 (1982).
20. Anderson, S. J. & Burr, D. C. *Vision Res.* **25,** 1147–1154 (1985).
21. Morgan, M. J. & Castet, E. *Nature* **378,** 380–383 (1995).
22. Collett, T. S. & Land, M. F. *J. comp. Physiol.* A **99,** 1–66 (1975).

ACKNOWLEDGEMENTS. We thank H. Barlow, D. Osorio and J. Anderson for comments and suggestions. R. Steel for donation of hive bees during winter. Supported by the EPSRC, BBSRC. The Swedish Natural Science Research Council and the British Council. N.J.B. was supported by a training fellowship from the Wellcome Trust.

CORRESPONDENCE and requests for materials should be addressed to D.C.O. (e-mail: dco1000@cam.ac.uk).

Abnormal processing of visual motion in dyslexia revealed by functional brain imaging

Guinevere F. Eden*, John W. VanMeter†, Judith M. Rumsey‡, José Ma. Maisog*, Roger P. Woods§ & Thomas A. Zeffiro||†

* Section on Functional Brain Imaging, NIMH, ‡ Child Psychiatry Branch, NIMH, || Laboratory of Diagnostic Radiology Research, OD, National Institutes of Health, Bethesda, Maryland 20892, USA
† Sensor Systems Inc., 103A Carpenter Drive, Sterling, Virginia 20164, USA
§ Department of Neurology, University of California at Los Angeles School of Medicine, Los Angeles, California 90098, USA

It is widely accepted that dyslexics have deficits in reading and phonological awareness[1,2], but there is increasing evidence that they also exhibit visual processing abnormalities that may be confined to particular portions of the visual system[3,4]. In primate visual pathways, inputs from parvocellular or magnocellular layers of the lateral geniculate nucleus remain partly segregated in projections to extrastriate cortical areas specialized for processing colour and form versus motion[5–10]. In studies of dyslexia, psychophysical[3] and anatomical[4] evidence indicate an anomaly in the magnocellular visual subsystem. To investigate the pathophysiology of dyslexia, we used functional magnetic resonance imaging (fMRI) to study visual motion processing in normal and dyslexic men. In all dyslexics, presentation of moving stimuli failed to produce the same task-related functional activation in area V5/MT (part of the magnocellular visual subsystem) observed in controls. In contrast, presentation of stationary patterns resulted in equivalent activations in V1/V2 and extrastriate cortex in both groups. Although previous studies have emphasized language deficits, our data reveal differences in the regional functional organization of the cortical visual system in dyslexia.

In the non-human primate brain, cells from the parvocellular and magnocellular subdivisions of the lateral geniculate nucleus (LGN) exhibit distinctive anatomical and physiological properties[11], and their projections remain partly segregated beyond the primary visual cortex. Neurons in the magnocellular layers (M-cells) have a phasic response and higher luminance contrast sensitivity, whereas neurons in the parvocellular layers (P-cells) have a more sustained response and sharper tuning, often opponent, to colour. In humans, homologous M-cell and P-cell systems have been identified on the basis of anatomical[12], psychophysical[13,14] and clinical evidence[15]. Further, evidence from functional neuroimaging studies has demonstrated regional functional specialization for visual motion processing in an extrastriate visual area (V5/MT)[16–19] that is thought to be dominated by input from the magnocellular stream. A defect in the M-cell pathway at the level of the LGN might be expected to result in impaired motion stimulus processing. Such a deficit should therefore be measurable psychophysically as an impaired ability to discriminate different stimulus velocities, or physiologically as impaired activation in MT/V5 during perception of moving visual stimuli.

Data suggesting that dyslexics have a selective deficit in the M-cell system include both psychophysical[3] and electrophysiological[4] differences in contrast sensitivity. Furthermore, post-mortem inspection of the LGN in dyslexic brains has indicated decreases in magnocellular neuron size, without differences in parvocellular layers[4]. Behavioural observations that some dyslexics have poor temporal judgement[20], visual instability[21], and higher coherent motion-detection thresholds[22] are consistent with a selective deficit in the M-cell system, but no direct neurophysiological demonstration of these deficits has been made.

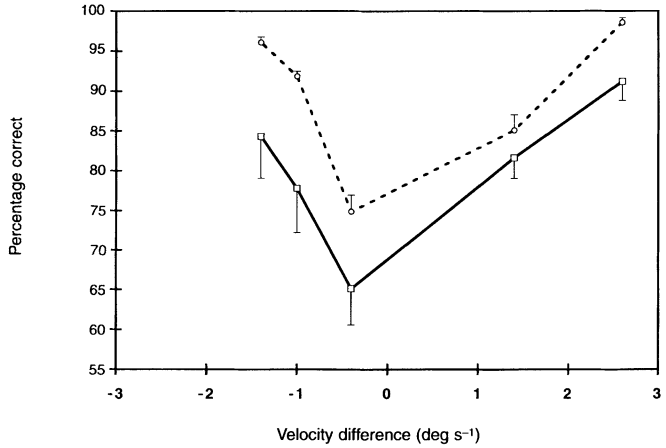

FIG. 1 Task performance is shown in a stimulus velocity detection task comparing the visual-motion sensitivity of six dyslexics (solid line) and six controls (broken line). The visual stimulus was the same as the M-stimulus used during fMRI data acquisition. Subjects saw low-contrast dots, moving horizontally with 100% coherence. Two such stimuli were presented in succession for 1 s each, the second differing from the first only in velocity. The subjects were instructed to state whether the second motion stimulus was slower or faster than the first. The first stimulus velocity was the same for all trials (7.0 deg s^{-1}) and the second stimulus velocity ranged form 5.6 to 9.6 deg s^{-1}. The dyslexics were significantly poorer in this task than the controls, showing reduced ability across the range of velocities tested (paired *t*-test, one-tailed, $P < 0.03$). The group mean for each stimulus pair is plotted with standard error bars.

We have tested the hypothesis that there is a selective M-cell-system processing deficit in dyslexia. Eight adult, male controls were carefully matched to six male dyslexics on IQ, age and other behavioural measures (Table 1). To assess whether there was a detectable visual-motion deficit in the dyslexic subjects, motion sensitivity was assessed by using a stimulus velocity judgement task. The results (Fig. 1) demonstrate a significant difference in performance between controls and dyslexics ($P < 0.03$).

Local blood-oxygenation level-dependent (BOLD[23,24]) contrast signals were measured by using fMRI, while the subjects viewed either a coherently moving, low-contrast (5%), random-dot stimulus (M-stimulus), or a stationary, high-contrast (40%), patterned stimulus (P-stimulus). Signal changes were assessed as in a previous experiment[19], by contrasting the motion condition to a fixation condition, and the pattern condition to a fixation condition. Because both the motion and the pattern stimulus were created from the same basic components (achromatic dark squares on a light background), we were able to equate the two comparisons in terms of their basic visual features. Area V5/MT was identified in each subject by its preferential sensitivity to motion (Fig. 2*a*).

Results of the single-subject analysis are shown in Table 2*a*. All control subjects exhibited bilateral motion sensitivity in a search volume surrounding the location of V5/MT[17]. In contrast, no activation was detected in any of the dyslexics in the same search volume, except for one subject's unilateral activation. A quite different result was observed with the stationary, pattern stimulus versus control comparison (Table 2*b*, *c*). Subjects in both groups exhibited similar responses to the pattern stimulus in both posterior occipital cortex (V1/V2; Table 2*b*) and in extrastriate visual areas (inferior temporal/fusiform gyrus; Table 2*c*), demonstrating that the differences in visual processing between groups were both regional and stimulus specific.

A group analysis of variance (ANOVA) confirmed the results of the single-subject analysis. Figure 2*b*–*e* depicts *t* maps of the two visual stimulation conditions, each compared to the control stimulus for both groups. In normal subjects (Fig. 2*b*), motion sensitivity was found bilaterally in the V5/MT area, and additional motion-sensitive areas were seen outside the search volume, posterior and anterior to V5/MT. In the dyslexic group (Fig. 2*c*) there was no activation in the area V5/MT, and a reduced response in other motion-sensitive areas. However, a comparison of the stationary pattern versus control stimuli revealed similar activation patterns in V1/V2 for both control (Fig. 2*d*) and dyslexic (Fig. 2*e*) groups.

Our results confirm previous demonstrations of robust motion sensitivity in V5/MT in normal subjects[17–19]. However, both individual and group analysis failed to detect responses to motion in dyslexics in this region, whereas normal responses to stationary, patterned stimuli were seen in V1/V2 and extrastriate visual areas. Further analysis confirmed that the activation differences between groups could not be attributed to higher signal intensities in V5/MT during the control condition. Because this study examined visual system function directly during a non-verbal condition, the observed differences could not be explained by the use of verbal strategies, which may be poorer in dyslexia[2].

Responses in other motion-sensitive, visual-cortical areas were detected in both groups, and raises the question of which mechanisms are responsible for the lack of activity in V5/MT. These temporal-lobe motion-sensitive areas have recently been reported to show particular sensitivity to coherent motion[19], and their different onset times have been characterized using fMRI in conjunction with magnetoencephalography[25]. The absence of motion sensitivity in V5/MT in dyslexics could result in a disruption of the normal coordinated temporal interaction with the other motion-processing areas. The results also raise the question of altered functioning of the non-geniculo-striate input to V5/MT (for example, from the superior colliculus and pulvinar) in dyslexia. Whatever the underlying mechanism, disruption of V5/MT activity may also interfere with re-entrant signals to other visual cortical areas (particular V1/V2), as well as to the oculomotor apparatus. This might explain the visual-motion-detection deficit demonstrated here, as well as previous reports of perceptual, oculomotor and evoked potential abnormalities in dyslexia[4,21].

In interpreting these findings, we must consider that, unlike patients with destructive lesions involving area V5/MT[15] and surrounding structures, the motion-detection deficit of dyslexics is subtle. Careful psychophysical testing is required for its detection, and it is rarely severe enough to cause symptomatic complaint. The visual-motion deficit we observed in dyslexia resembles that seen in non-human primates after recovery from focal MT lesions. Although injection of ibotenic acid into V5/MT causes severe, acute motion-detection deficits, motion sensitivity recovers over a period of days to weeks. The animals eventually show only minimal impairment of motion detection, despite a complete absence of neurons in area V5/MT[26]. Although focal ischaemic lesions of V5/MT can cause severe and permanent motion-detection deficits, it is possible that the ibotenic-acid

TABLE 1 Behavioural profile of subjects

	Controls ($n = 8$) (means (s.d.))		Dyslexics ($n = 6$) (mean (s.d.))		*t*-test
Chronological age (years)	25.5	(6.2)	26.8	(6.2)	n.s.
Education (highest level completed)	15.4	(2.7)	13.6	(1.4)	n.s.
Hollingshead's Socio-economic status	52.5	(27.6)	71.3	(21.9)	n.s.
Handedness	98.7	(3.3)	98.7	(3.3)	n.s.
Attention deficit disorder	0		0		n.s.
Wechsler adult intelligence scale-revised IQ					
Verbal	115.7	(16.4)	109.5	(9.1)	n.s.
Performance	106.7	(14.6)	115.5	(9.4)	n.s.
Full	112.7	(14.7)	114.0	(5.3)	n.s.
Wide range achievement test III					
single word reading	111.85	(4.9)	89.3	(11.8)	$P < 0.001$
spelling	107.4	(6.1)	69.8	(15.8)	$P < 0.001$
mathematics	112.7	(10.5)	93.8	(12.6)	$P < 0.005$
Gray oral reading test III					
rate	14.3	(1.4)	5.3	(2.9)	$P < 0.001$
accuracy	13.6	(2.4)	3.3	(2.2)	$P < 0.001$
passage score (decoding)	14.3	(1.8)	4.7	(2.4)	$P < 0.001$
Phonological skills (pseudo-word reading)	51.2	(4.8)	40.8	(2.6)	$P < 0.001$

All subjects were monolingual, adult American males, without neurological abnormalities. All were strongly right-handed (at least 92% on the handedness portion of the physical and neurological examination for subtle signs, and had no history of attention deficit disorder using the DSM-III-R criteria. Normal controls were closely matched to dyslexics on gender, age, education, socio-economic status and IQ. Reading was assessed with the Wide range achievement test (3rd edn) and the Gray oral reading test 3rd revision (GORT3). The dyslexic subjects met all of the following criteria: (1) a documented childhood history of reading disability; (2) an absolute reading deficit (below 8 points on the passage score of the GORT3); and (3) a discrepancy of at least 2 standard deviations between their reading (on the passage score of the GORT3) and verbal IQ (Wechsler adult intelligence scale-revised). The dyslexics demonstrated significantly poorer phonological awareness than controls on a pseudo-word (non-word) reading task (Goldman-Fristoe-Woodcock's reading of symbols). n.s., Not significant.

TABLE 2 Local voxel maxima

	Left				Right			
	Talairach coordinates (mm)				Talairach coordinates (mm)			
Subjects	*x*	*y*	*z*	*z*-score	*x*	*y*	*z*	*z*-score
(*a*) In V5/MT for motion versus fixation contrast								
Controls								
C1	−62	−72	+10	4.5	+58	−62	+12	5.6
C2	−64	−78	+10	5.6	+56	−68	+2	4.6
C3	−48	−84	+4	6.4	+34	−84	+2	7.6
C4	−50	−64	+8	5.3	+60	−62	+8	5.1
C5	−32	−74	+10	4.7	+52	−64	+6	4.2
C6	−60	−66	+10	5.3	+44	−78	+2	5.7
C7	−58	−74	−4	4.4	+52	−76	+2	5.7
C8	−44	−86	+12	6.9	+44	−66	+4	6.4
Dyslexics								
D1				n.s.				n.s.
D2				n.s.				n.s.
D3				n.s.				n.s.
D4				n.s.				n.s.
D5	−42	−62	+8	5.6				n.s.
D6				n.s.				n.s.
(*b*) In V1/V2 for pattern versus fixation contrast								
Controls								
C1	−12	−82	−8	7.6	+14	−90	−10	5.6
C2	−6	−82	0	4.8	+6	−96	+2	4.7
C3	−4	−76	+2	7.3	+22	−88	+14	6.1
C4	−24	−74	+6	6.0	+28	−74	+8	4.2
C5	−22	−92	+12	4.1	+6	−96	+10	4.9
C6	−22	−104	+4	4.1				n.s.
C7				n.s.	+18	−96	+4	4.3
C8	−14	−94	+8	5.1			ns	
Dyslexics								
D1	−16	−98	−2	5.9	+16	−94	−4	5.4
D2	−18	−88	+2	4.4				n.s.
D3	0	−105	+6	4.1	0	−105	+6	4.1
D4	−24	−70	−6	4.2	+6	−82	−6	5.5
D5	−2	−96	0	4.6	0	−106	+2	4.1
D6	−24	−80	+8	8.1	+6	−78	+10	6.5
(*c*) In extrastriate cortex (inferior temporal/fusiform gyrus) for pattern versus fixation contrast								
Controls								
C1	−58	−48	−16	6.1	+58	−48	−16	5.7
C2	−62	−42	−6	4.4	+46	−48	−6	5.1
C3	−48	−32	−10	6.4	+50	−40	−27	5.3
C4	−64	−48	−8	4.9	+64	−32	−8	4.0
C5				n.s.	+54	−48	−24	4.7
C6				n.s.				n.s.
C7	−46	−32	−14	4.0	+54	−32	−12	4.7
C8				n.s.				n.s.
Dyslexics								
D1	−64	−32	−14	5.4	+64	−32	−14	5.4
D2	−58	−49	−18	4.1				n.s.
D3	−40	−42	−6	4.1	+50	−32	−14	4.4
D4				n.s.				n.s.
D5	−52	−44	−16	4.3	+52	−42	−12	4.6
D6	−38	−44	−8	4.2	+48	−36	−24	4.5

Single-subject analysis, showing the locations in the Talairach atlas[27] for the most significantly activated voxels in response to: (*a*) the motion stimulus in V5/MT; (*b*) the stationary pattern stimulus in V1/V2; and (*c*) the stationary pattern stimulus in extrastriate object/form area[28] in normals and dyslexics. The time series for each of these voxels was examined to confirm that the signal changes were related to the task. As our interest was specific to area V5/MT, the search for areas sensitive to motion was confined to a volume containing the Talairach[27] coordinates reported to contain V5/MT[17] (*x*, lateral to +30 or −30; *y*, posterior to −62; *z*, between −4 and +12 in the inferior/superior direction). The borders for V1/V2 were determined using the Talairach atlas[27]. Spatial normalization of the functional images allowed accurate neuroanatomical localization for single-subject analysis as well as intersubject averaging for the group study. MEDx (Sensor Systems, Herndon, VA) was used for image analysis and visualization. The matrices from the following transformations were concatenated and applied to the original echo planar imaging (EPI) data[29]. (1) The EPI data from each scan were co-registered with a 6 degrees-of-freedom (d.o.f.) transformation[30] to correct for interscan head motion. (2) Geometric spatial distortions caused by magnetic field inhomogeneities were corrected with a 12 d.o.f. transformation by registering the EPI images to a coplanar conventional volume, acquired during the same session (spoiled grass gradient recalled echo (SPGR): field of view (FOV), 32 cm; acquisition matrix, 256 × 256; slice thickness, 5.0 mm; echo time (TE), 9 ms; repetition time (TR), 150 ms; 30 contiguous coronal slices). (3) A high-resolution conventional scan was acquired on a separate day (SPGR: FOV, 24 cm; acquisition matrix, 512 × 512; slice thickness, 1.5 mm; TE, 5 ms; TR, 24 ms; 124 sagittal slices). High-resolution scans were spatially normalized into the Talairach space[27] by identifying the locations of the anterior and posterior commissures (AC–PC line) and applying a second-order polynomial transformation. (4) The coplanar SPGR volume was registered to the high-resolution SPGR volume. In this way EPI images were transformed into Talairach space, resulting in stereotactically normalized EPI data from which *t*- and *z*-score maps were computed.

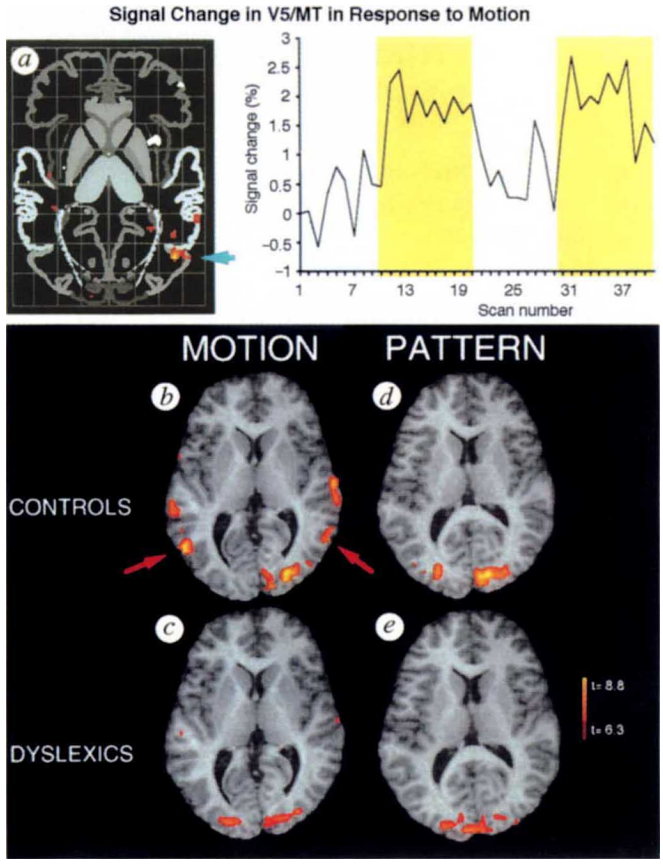

FIG. 2 *a*, Left, a single control subject's brain after spatial normalization[27], and calculation of *z*-maps. Right, graph shows changes in image intensity in the most significantly activated, single voxel located in right area V5/MT. Activation for V5/MT is only displayed for the right hemisphere, as V5/MT on the left side lies in a more superior axial plane. The transverse image shows V5/MT located at Talairach coordinates $x = +44$, $y = -66$, and $z = +4$, which also corresponds to the most common anatomical location of V5/MT, at the ascending limb of the inferior temporal sulcus[17,18]. *b*–*e*, For group comparisons, hypothesis testing was performed using an ANOVA and planned contrasts for each group in the two conditions. Statistical maps are displayed on one subject's spatially normalized MRI, shown at transverse planes $z = +8$ and $z = +10$ relative to the AC–PC line, for the motion stimulus versus control (*b*, *c*) and pattern stimulus versus control (*d*, *e*) contrasts. V5/MT can clearly be seen in the control group (*b*) but not in the dyslexic group (*c*) by its preferential activation in the moving-stimulus condition. In contrast, both groups (*d*, *e*) show similar responses in area V1/V2 to the stationary, high-contrast, patterned stimulus. In the motion condition, additional motion-sensitive areas can be seen in the control group (*b*) at anterior temporal as well as posterior areas. Neuroimaging studies of motion sensitivity have proposed the latter area to be V3 (refs 18, 19). Both of these areas were also identified, to a lesser extent, in the dyslexic group. All images are presented in the neurological convention (subject left, image left).

METHODS. Data are derived from multislice EPI data of local BOLD[23,24] contrast signals, on a GE Signa 1.5 Tesla system with two surface coils positioned in an oblique orientation surrounding the occiput. Contiguous coronal 5-mm slices (30), 32 cm; acquisition matrix, 64×64; TE, 40 ms; TR, 10 s) were collected, resulting in a volume of 5-mm cubic voxels that spanned occipital and posterior parietal cortex; 90 scans were obtained for each subject. During the scans, subjects maintained fixation while viewing: (1) a fixation cross on a field of uniform illumination; (2) a low-contrast (Michaelson contrast, 5%), array of black dots on a grey background, all moving at 100% coherence in one of eight directions at a speed of 10 deg s^{-1} (M-stimulus); or (3) a high-contrast (40%), stationary, patterned dot field with high spatial correlation, resulting in texture (P-stimulus). All three stimulus had equal luminance, moving and stationary pattern stimuli had the same global spatial frequency. Each dot (square) subtended 1°. All subjects reported perceiving motion in (2). Stimuli were presented on a back-projection screen, and the display covered 30° of the horizontal and 20° of the vertical central visual field. Blocks of 10 trials of viewing one of the three stimuli were presented, and repeated to yield 90 scans (123123123). A 1-min interscan interval minimized temporal autocorrelation and neural habituation. After ratio normalization, task-related signal changes were detected by computing voxel-wise *t*-statistic maps contrasting motion versus fixation to detect motion sensitivity, and stationary pattern versus fixation to detect pattern sensitivity. After transformation to the standard normal distribution, areas exhibiting motion or pattern sensitivity were identified using *z*-score ≥ 4 ($P < 0.00003$) as the critical threshold. After correction for multiple comparisons with reference to the search volume used, the critical threshold for the V5/MT volume was $P < 0.003$, and the threshold for the V1/V2 volume was $P < 0.01$.

lesion is a better model of the developmental lesion that may result in the visual-motion detection impairment observed in dyslexia.

We have demonstrated the feasibility of using fMRI to detect and localize abnormal neuronal processing in dyslexia. Our findings provide a neurophysiological basis for the previously observed visual perceptual processing deficits in dyslexia that have implicated the M-cell system. These visual-system abnormalities may be one component, and therefore a marker, of a disorder that embodies numerous constituents, including the well-studied deficit in phonological awareness[1,2]. Their joint appearance in dyslexia may be due to the presence of an underlying deficit in systems that have in common the processing of temporal properties of stimuli. This deficit may manifest itself as disorders of phonological awareness, rapid naming, rapid visual processing, or motion detection. □

Received 26 January; accepted 17 May 1996.

1. Bradley, L. & Bryant, P. *Nature* **271,** 746–747 (1978).
2. Snowling, M. *Psychol. Res.* **43,** 219–234 (1981).
3. Lovegrove, W. J., Bowling, A., Badock, D. & Blackwood, M. *Science* **210,** 439–440 (1980).
4. Livingstone, M., Rosen, G. D., Drislane, F. W. & Galaburda, A. *Proc. natn. Acad. Sci. U.S.A.* **88,** 7943–7947 (1991).
5. Zeki, S. M. *Brain Res.* **53,** 422–427 (1973).
6. Ungerleider, L. G. & Mishkin, M. in *Analysis of Visual Behavior* (eds Ingle, D. J., Goodale, M. A. & Mansfield, R. J. W.) 549–586 (MIT Press, Cambridge, MA, 1982).
7. Livingstone, M. & Hubel, D. *Science* **240,** 740–749 (1988).
8. Maunsell, J. H. R. & Newsome, W. *A. Rev. Neurosci.* **10,** 363–401 (1987).
9. Van Essen, D. & Maunsell, J. H. R. *Trends Neurosci.* **6,** 370–375 (1983).
10. Zeki, S. M. & Shipp, S. *Nature* **335,** 311–317 (1988).
11. Shapley, R. & Perry, V. *Trends Neurosci.* **9,** 229–235 (1986).
12. Clarke, S. & Miklossy, J. *J. comp Neurol.* **298,** 188–214 (1990).
13. Kaplan, E. & Shapley, R. *J. Physiol., Lond.* **330,** 125–143 (1982).
14. Kulikowski, J. & Tolhurst, D. *J. Physiol., Lond.* **232,** 149–162 (1973).
15. Zihl, J. *Brain* **106,** 313–340 (1983).
16. Corbetta, M., Miezin, F. M., Dobmeyer, S., Shulman, G. L. & Petersen, S. E. *Science* **248,** 1556–1559 (1990).
17. Watson, J. D. G. *et al. Cerebr. Cortex* **3,** 79–94 (1993).
18. Tootell, R. *et al. J. Neurosci.* **15,** 3215–3230 (1995).
19. Cheng, K., Fujita, H., Kanno, I., Miura, S. & Tanaka, K. *J. Neurophysiol.* **74,** 413–427 (1995).
20. Eden, G., Stein, J., Wood, H. & Wood, F. *Cortex* **31,** 451–469 (1995).
21. Eden, G., Stein, J., Wood, H. & Wood, F. *Vision Res.* **34,** 1345–1358 (1994).
22. Cornelissen, P., Richardson, A., Mason, A., Fowler, S. & Stein, J. *Vision Res.* **35,** 1483–1494 (1995).
23. Ogawa, S. *et al. Proc. natn. Acad. Sci. U.S.A.* **89,** 5951–5955 (1992).
24. Kwong, K. K. *et al. Proc. natn. Acad. Sci. U.S.A.* **80,** 5676–5679 (1992).
25. Dale, A. *et al. Soc. Neurosci. Abstr.* **21,** 10 (1995).
26. Newsome, W. T. & Paré, F. B. *J. Neurosci.* **8,** 2201–2211 (1988).
27. Talairach, J. & Tournoux, P. *Co-planar Stereotaxic Atlas of the Human Brain* (Thieme, New York, 1988).
28. Sergent, J., Ohta, S. & MacDonald, B. *Brain* **115,** 15–36 (1995).
29. Zeffiro, T. A., Eden, G. F., Woods, R. P. & vanMeter, J. W. *Adv. exp. med. Biol.* (in the press).
30. Woods, R. P., Cherry, S. R. & Mazziota, J. C. *J. Comput. assist. Tomogr.* **16,** 620–633 (1992).

ACKNOWLEDGEMENTS. We thank P. Jezzard, J. Haxby and L. Ungerleider for discussions, and C. Moonen and the NIH *in vivo* NMR Center for use of their facilities. This work was supported by a grant from the Human Science Frontier Program. G.F.E. was supported by a Fogarty fellowship, sponsored by Judith Rapoport.

CORRESPONDENCE and requests for materials should be addressed to G.F.E. (e-mail: eden@alw.nih.gov).